atmosphere

MDPI

Article

Fugitive Emissions from Mobile Sources—Experimental Analysis in Buses Regulated by the Euro 5 Standard

Antonio C. Caetano [1,*], Alexandre M. S. da Costa [1], Vanderly Janeiro [1], Paulo H. Soares [2], Leonel R. Cancino [3] and Cid M. G. Andrade [1,*]

[1] Department of Mechanical Engineering, State University of Maringá, Maringá 87020-900, PR, Brazil
[2] Department of Informatics, Federal Technological University of Paraná, Guarapuava 85053-525, PR, Brazil
[3] Internal Combustion Engines Laboratory (LABMCI), Joinville Technological Center (CTJ), Federal University of Santa Catarina (UFSC), Rua Dona Francisca 8300, Joinville 89219-600, SC, Brazil
* Correspondence: accaetano.ac@gmail.com (A.C.C.); cmgandrade@uem.br (C.M.G.A.); Tel.: +55-4499115-7333 (C.M.G.A.)

Abstract: Fugitive emissions are unintentionally produced by pipeline leakage and evaporation in industrial processes and contribute 5% of Global Greenhouse Gas emissions (GHG). Frictional wear and thermal fatigue in vehicle exhaust pipe couplings and joints can cause leaks that are not visible and difficult to quantify. It is therefore essential to trace and document these sources. In this work, an experimental survey was conducted on buses in accordance with Regulation (EC) N° 715/2007 of the European Parliament. Statistical methods by means of a priori analysis aided by G*Power 3.1 software was used to define the required sample. Three random sample groups were stratified and fugitive gases were encased and piped into a bronze tube 5 mm in diameter and 500 mm in length. A Horiba PG-300 analyzer was used to analyze the samples using chemiluminescence and infrared methods. The results proved the existence of fugitive emissions in all samples analyzed with variations of (3.000–27.500 ppm) among the samples for CO_2, (6.0–138.5 ppm) and (2.0–5.0 ppm) for CO and NO_x, respectively. Statistical analysis showed that engine mileage had no significant influence on NO_x emissions, while CO and CO_2 emissions increased with mileage. Analysis using Response Surface Methodology (RSM) indicated a trend of increasing concentrations of CO_2 and CO for both explanatory variables, mileage and usage time.

Keywords: fugitive emissions; atmospheric emissions; Greenhouse Gases; mobile fonts; exhaust pipe; Carbon dioxide; Carbon monoxide; Nitrogen oxide; buses

Citation: Caetano, A.C.; da Costa, A.M.S.; Janeiro, V.; Soares, P.H.; Cancino, L.R.; Andrade, C.M.G. Fugitive Emissions from Mobile Sources—Experimental Analysis in Buses Regulated by the Euro 5 Standard. *Atmosphere* **2023**, *14*, 613. https://doi.org/10.3390/atmos14040613

Academic Editor: Jacek Koziel

Received: 21 January 2023
Revised: 21 February 2023
Accepted: 8 March 2023
Published: 23 March 2023

1. Introduction

Estimates of global Greenhouse Gas (GHG) emissions based on current nationally declared mitigation ambitions under the Paris Agreement would bring the emissions amount to the 52–58 $GtCO_{2-eq}$ [1] level. Attempting to find solutions to mitigate the effects of atmospheric emissions on the climate, leaders of various nations meet frequently with the common purpose of encouraging and guiding the people of the world to become aware of and preserve the environment for the sustainable subsistence of generations of humans, wildlife and flora. At the first major conference in Stockholm in 1972, twenty-six principles and one hundred and nine recommendations directed the first global policies to address climate issues [2]. Agenda 21, established in the Rio 92 Declaration [3] brought important advances in preparation for the 2015 Paris Agreement [4] that culminated in the elaboration of twenty-nine articles with recommendations for the member countries. The second article of the Paris Agreement states that the global average temperature increase should be kept within 2 °C of pre-industrial levels, with efforts to limit this temperature increase to no more than 1.5 °C above pre-industrial levels.

When analyzed by sectors, the actions to combat the emission of pollutants show good results. 45 randomly analyzed countries reduce their emissions by 25.7% in 2020 with a

1990 base year [5]. With a 21% reduction in the same period, the European Union showed similar performance [6]. However, at the global level, the volume of GHG emissions is still high and may overshadow the achievement of the goals set out in the Paris Agreement. In 2019, global net anthropogenic GHG emissions were 12% higher than 2010 [7] and 54% higher when compared to the 1990 base year. This behavior can be explained by the increase in the annual average of GHG emissions in the decade 2010–2019 that was 16.2% higher than the annual average of the previous decade, which represents an absolute increase of 56 $GtCO_{2-eq}$.

Fugitive Emissions

Classified by the IPCC as code 1B, fugitive emissions are the unintentional release of gases during the extraction, processing, transport and discharge of fossil fuels, fugitive emissions contribute significantly to GHG emissions [8]. The IPCC's sixth assessment report (AR6) states that the energy sector, through the production and transport of fossil fuels accounted for 18% of global GHG emissions in 2019. Among the most significant species, methane (CH_4) emissions accounted for 32% of this total. Considering all sources, fugitive emissions accounted for 6% of total GHGs in the same year. In absolute numbers, oil and gas production and transportation generated a total of 2.6 $GtCO_{2-eq}$ in fugitive emissions in 2020, while mining activities contributed 1.3 $GtCO_{2-eq}$ in the same year [9]. Data available from the United Nations Framework Convention on Climate Change (UNFCCC) Inventory, (Annex I countries) show that in 2016, fugitive emissions generated by industrialized countries were 1.33 billion tons of CO_{2-eq}, this represents an 85% increase when compared to 1990 data. The report emphasizes the importance of politics that mitigate fugitive emissions, which, according to the study, represents 5% of total GHG emissions [10]. The difficult monitoring of fugitive emissions is a complicating factor for effective estimates and causes uncertainty in activity data (AD) statistics. Covering 93 countries and covering 97% of fugitive emissions, the IPCC-06 estimates (with a confidence level of 95%) that fugitive emissions caused by the combustion of fossil fuels (1.B.2—gas and oil) is 10% and 20% for industrialized and developing countries, respectively [11]. Despite the apparent expressiveness in the indicators, this number can be much higher. In Nigeria, an estimate based on the Intergovernmental Panel on Climate Change IPCC-2006 (base year 2012) projected to 2027, revealed that flaring of waste gas in oil production contributes 75.27% of fugitive emissions in the oil and gas sector when compared to other sectors [12]. To attenuate the serious problem, the study suggests that the Nigerian government compel oil companies to channel their flared gases to power plant, making them reusable. Estimates indicate that methane emissions from oil and gas operations, despite the emergence of new data from satellites and other measurement campaigns, are underestimated by about 25% to 40% [13]. The Clean Development Mechanism (CDM) is based on offsetting CO_2 through projects that developing countries can design and implement to earn saleable credits equivalent to the amount of CO_2 they reduce. A wide range of such projects can qualify under the CDM criteria, from wind energy projects to projects credited for destroying waste and industrial gases [14]. A critical assessment of CDM projects implemented to reduce fugitive emissions during industrial activities was conducted and found that only 1.98% out of a total of 7.749 CDM projects had been effectively implemented by 2016 in India [15]. The 154 implemented projects contributed with a reduction of 8.87% in GHG emissions, which represents a total of 1.66 $MtCO_{2-eq}$ in estimated fugitive emissions across all CDM sectors.

The transportation sector, a subset of the energy sector, ranks highest in pollutant emissions. In São Paulo, infrared photoacoustic spectroscopy analysis was used to detect emissions at four bus terminals. With averages of 546 ppm, 526 ppm, 525 ppm and 516 ppm CO_2 at both terminals, the samples were compared with previous studies and showed that the newer lifetime bus fleet emitted fewer pollutants compared to older vehicles [16]. The major contribution to GHG emissions from the internal combustion engine is CO_2. Other GHG gases (such as $N2O$, CH_4 make up a significantly smaller proportion [17]). It should

be noted that CO_2 emissions in internal combustion engines do not depend much on the air pollution reduction measures implemented, the main potential for reducing them is lower fuel consumption [18]. However, better fuel consumption technologies are not capable of zeroing pollutant emissions, in this sense, it is necessary to adopt measures to treat the gases in the catalyst (after-treatment gas system). In Curitiba and Maringá, important cities in southern Brazil, the concentration of pollutants in regions near bus traffic was monitored by means of autonomous and independent sensors. In Curitiba, the study detected a high spatial variability of particulate matter along the bus route and concluded that there is a direct influence of bus transportation on the concentration of pollutants in the region. 829 ppm detected in an analysis carried out in Maringá, reveals that the air is 38% more polluted than the average considered safe for humans [19,20]. Although there is some scientific data on pollutant emissions in activities related to passenger transportation, there is a scarcity of studies on fugitive emissions from mobile sources, making even more rare or non-existent research that has investigated leaks in exhaust pipes of trucks and buses.

Attempting to contribute to this field, this work is characterized by a pioneering analysis of possible leakage of exhaust gases in exhaust pipes of buses regulated by the Euro 5 standard in accordance with Regulation (EC) N° 715/2007 of the European Parliament [21].

2. Theoretical Background (Leakage Measurements/Sample and Population Size)

Increasingly sophisticated analytic techniques are used by researchers to obtain the optimal population size (N) and thus generate maximum likelihood and representativeness fits in each model to produce sufficiently accurate reliability coefficients for a sample size that adequately represents the population. to obtain the optimal population size, N, and thus generate maximum likelihood and representativeness fits in each model to produce sufficiently accurate reliability coefficients for a sample size that adequately represents the population. The most parsimonious model is required that involves the least possible number of parameters to be estimated and that explains well the behavior of the response variable and seeks an acceptable convergence between the model and the empirical data. Reproducibility and representativeness based on meta-analyses and meta-regressions in $N \geq 25$ was developed in an experimental study for economic, medical, epidemiological, ecological and biogeographical analyses [22]. Sample size calculation using discrete Weibull methodology for distribution skewness, covariance structure and number of zeros with accurate sample size results by means of negative binomial Poisson regression also showed good results in previous studies [23].

The methodology for monitoring and estimating leakage in valves, flanges, pump seals, open lines and other components that are part of the process of transporting gases in pipelines is detailed by the U.S. Environmental Protection Agency (EPA) [24]. Although it does not make references to mobile source gas collection practices. The EPA Method 21 [25] indicates the encapsulation system as an option for collecting fugitive gases in leaky pipelines. Based on EPA Method 21, researchers have developed optical gas imaging (OGI) technology for use in detecting leaks of volatile organic compounds (VOCs) in equipment. The results showed that faster detection may help in monitoring an area rather than just one component, and this methodology may be an indication of more effective use than EPA Method 21 [26]. In another study, researchers used leak detection methods for volumetric emissions obtained by direct measurement using HFS that consider leak rates greater than 200 g/h were applied using vacuum trapping techniques on a leaky control valve [27].

A sample design and definition of the optimal sample population size (N) that represents reliable data is crucial in experimental research. The software G*Power 3.1 was used in previous research to calculate the minimum sample size and data analysis with Pearson correlation test of linear regression with covariate adjustment [28]. In another study, effect size of 0.92, power of 0.999, and confidence index in 5% was determined by G*Power 3.1 to examine the influence of transcranial cerebellar direct current stimulation on non-motor (cerebellar) symptoms in patients, and to explore the time course of these effects [29]. With a significance level at 5% and power of 80% the program G*Power 3.1 was used to define

sample size in a study to find the reasons for rejection of medication use and to determine the wastage rate and financial consequences [30].

3. Materials and Methods

In order to better contribution with the climate change appeal, measurements in the exhaust pipeline of buses (urban and intercity buses) were performed. The buses are operating at Boa Vista and Manaus towns, at the north of Brazil. Details about the measurement techniques, sampling and experimental procedures are given as follows.

3.1. Defining and Implementing the Sample Model

In this research statistical methods by means of analysis aided by the free software G*Power 3.1 was adopted. The sample size whose definition of efficiency of 0.9, power of 83% and level of significance of 5%, indicates the amount of 10 samples, as satisfactory for significantly relevant answers.

3.2. Experimental Procedure

To collect the fugitive gases, during one week, technical visits were made to three passenger transportation companies in the cities of Manaus, Amazonas (BRA) and Boa Vista, Roraima (BRA). Ten buses were selected and divided into three categories. Figure 1 shows a representation of the bus models used by operational category and engine, the specifications are as follows. Figure 1a Light Diesel Engine (LDV) for Urban Passenger Transport—Diesel engine, 7.2 L, vertical, forward, fully electronic, fuel injection with "commom rail" technology, 6 cylinders in line, turbocharged and intercooled, self-protected against overheating. Emissions level in accordance with CONAMA regulation Phase Vll (EURO V). Lk39 air compressor. Butterfly-type engine brake [31]; Figure 1b Heavy articulated bus (HDV) for urban passenger transport. Emission level Euro 5 Injection system Injection pump Capacity dm^3 12.1 Cylinders 6 in line Max. power hp/ISO power kW 340/250 Max. torque ISO 1585 Nm 1700 Engine torque speed rpm 950–1400 [32]; Figure 1c Heavy passenger intercity transport bus (HDV). Euro emission standard, SCR engine system, Common Rail SCR, Common Rail Displacement dm^3, 11 Cylinders/array of 6/inline inlet 6/inline inlet [33].

In order to reduce the possible kinetics sample gas evolution, a copper tube 5000 mm long and 5 mm in diameter was connected to the exhausts of the vehicles, Figure 2. The longer the copper tube, the lower the chance of kinetic evolution due to the heat transfer process (sample gas-copper tube wall). It is worth noting that the sampling location was not the same for all the buses involved in this research, the sampling location was selected in function of visual inspection in the exhaust gas pipeline, along the tube among the exhaust valve port and before the after-treatment gas system, for each one of the ten buses, as shown in Figure 2. For better efficiency of the enclosure, an aramid adhesive tape that has high thermal resistance was used as thermal insulator. Overlaid on the aramid, another tape (Torofita) was used as a physical barrier to minimize possible gas leaks and to prevent external oxygen from entering the samples, which could alter the composition of the chemical species and cause inconsistencies in the results. The collected fugitive gases were stored in 1-liter capacity containers and later sent for laboratory analysis. Related to the end of the cooper tube was designed to fit the inlet of the sampling bag valve. The sampling bags made up of polyvinyl fluoride film (Tedlar®). In order to not interfere in the mass flow rate throughout the leakage area, pump was not used, the sampling bags were filled by the pressure difference among the enclosured leakage area and the ambient pressure (acting in the wall of the bags). All the bags came at vacuum (with no air inside) from the laboratory were analyzes were performed.

Figure 1. Illustrative images of the bus models used in this research. (**a**) Light Diesel Engine (LDV) for Urban Passenger Transport, (**b**) Heavy articulated bus (HDV) for urban passenger transport, (**c**) Heavy passenger intercity transport bus (HDV).

Figure 2. Encapsulation of gases using high-strength aramid tape aided by torofita: (**a**) Dark color, indicating possible gas leakage; (**b**) Enclosed location with gases channeled through pipes; (**c**) Sample collecting container, receiving the channeled cases.

3.3. Criteria and Reference Conditions Used for Gas Sampling

Enclosure for gas collection is a methodology used in exceptional cases but represents good consistency when compared with results obtained in an analysis that considers the total gas flow. Based on the studies cited, in this research was diverted a small portion of the undiluted exhaust gas into collection containers. It should be noted that, that small gas portion represent the gas flow throughout the leakage area (fugitive emissions). The flow obtained for a time interval, as far as possible, was proportional to the total flow in the same time interval. Three random sample groups were stratified, Figure 1. The gases were collected with the engines in operation, with temperature and pressure similar to the real work regime, but with torque (hp) and displacement (m) in zero position. The information about parameters and working conditions of the engines are presented in Tables 1–3, which include the values of mileage (km), engine speed (rpm), sampling collection time (s), wall tailpipe temperature °C and engine working temperature °C.

Table 1. Engine parameters and operating conditions along gas sampling. Steady state and working temperature similar to the on-load state—B340M.

Production year	Mileage (km)	Rotation (rpm)	Power (cv/kW)	Gas Sample Collection Time (s)	Engine * Temperature (°C)	Wall † Temperature (°C)	Transport Category
2014	518,640	1700	340/250.07	664	93.1	175.0	Urban
2014	367,100	1700	340/250.07	721	92.4	155.0	Urban

* Data collected from the on-board bus control panel; † External wall temperature measured in the exhaust gas pipeline.

Table 2. Engine parameters and operating conditions along gas sampling. Steady state and working temperature similar to the on-load state—B270F.

Production year	Mileage (km)	Rotation (rpm)	Power (cv/kW)	Gas Sample Collection Time (s)	Engine * Temperature (°C)	Wall † Temperature (°C)	Transport Category
2012	846,694	1700	270/198.58	788	87.0	110.0	Urban
2012	367,100	1700	270/198.58	602	86.0	103.7	Urban
2013	518,640	1700	270/198.58	540	88.0	106.0	Urban
2013	367,100	1700	270/198.58	781	85.0	104.6	Urban

* Data collected from the on-board bus control panel; † External wall temperature measured in the exhaust gas pipeline.

Table 3. Engine parameters and operating conditions along gas sampling. Steady state and working temperature similar to the on-load state—B450R.

Production year	Mileage (km)	Rotation (rpm)	Power (cv/kW)	Gas Sample Collection Time (s)	Engine * Temperature (°C)	Pipeline Wall † Temperature (°C)	Transport Category
2015	670,803	1700	450/330.97	660	96.0	137.0	Road
2016	856,794	1700	450/330.97	664	92.0	104.0	Road
2018	938,933	1700	450/330.97	605	94.0	152.0	Road
2020	93,449	1700	450/330.97	721	91.8	132.0	Road

* Data collected from the on-board bus control panel; † External wall temperature measured in the exhaust gas pipeline.

4. Results

The ten collected bag samples were sent to the laboratories of the company White Martins in São Paulo, where they were analyzed using an analyzer (Horiba PG-300) that can measure simultaneously up to five gas components, separately. The PG-350 software runs under Windows (Vista, XP, 7 and higher), provides a simple interface to acquire data and save CSV files and allows connection to any network, its line selection valve NO and NO_x can be controlled and switched automatically during its data acquisition. To analyze the NO_x concentrations the cross-flow modulation chemiluminescence detection method. CO_2, SO_2 and CO were analyzed by the non-dispersive infrared modulated cross-flow absorption method. The results generated by the analysis of the samples were provided by the laboratory by official certificate under identification N° 041/21 of technical responsibility of CRQ IV Region N° 04266629. The variables time (s) and mass (kg) were used to calculate the mass flow rate needed to fill the containers with sample gases, Equation (1).

$$Q_m = \frac{m}{t} \tag{1}$$

where m is the mass (kg), t the time (s) and Q_m the mass flow rate (kg/s). Considering the particularity of this research, Table 4 was generated from Equation (1) and can be used as a basis for replication for future works.

Table 4. Flow rate in seconds calculated based on the experimentally collected data.

Vehicle	Mass (kg)	Time (s)	Mass Flow Rate (kg/s)
A	0.011	788	1.396×10^{-5}
B	0.017	540	3.148×10^{-5}
C	0.027	602	4.485×10^{-5}
D	0.015	781	1.921×10^{-5}
E	0.029	664	4.637×10^{-5}
F	0.023	721	3.190×10^{-5}
G	0.024	605	3.967×10^{-5}
H	0.090	664	1.355×10^{-5}
I	0.011	660	1.667×10^{-5}
J	0.012	721	1.664×10^{-6}

Unit of Measure Transformation

Vehicle exhaust emissions are usually measured using a gas analyzer whose results are reported in Parts Per Million (ppm), however, it is important to compare these emissions with European standards which are usually reported in (g/kWh) for heavy duty vehicles and (g/km) for light duty vehicles. For the purpose of comparison with the European standard we use the Equations (2) and (4) based on empirical constants reported in previous studies [34–37] whose results are available in Table 5 and Figure 3.

$$CO(\mathrm{g/kWh}) = 35.91 \times CO(vol\%) \tag{2}$$

$$NO_x(\mathrm{g/kWh}) = 6.636 \times 10^{-3} \times NO_x(\mathrm{ppm}) \quad (3)$$

$$CO_2(\mathrm{g/kWh}) = 63.47 \times CO_2(vol\%) \quad (4)$$

Table 5. Concentration of fugitive gases analyzed in the laboratory. Values converted to (g/kWh).

Vehicle	Model	Year	Mileage (km)	*CO* * (g/kWh)	CO_2 * (g/kWh)	NO_x * (g/kWh)
A	B270F	2012	846,694	$4.97 \times 10^{-1} \pm 4.9 \times 10^{-3}$	171.3 ± 1.7	$1.86 \times 10^{-2} \pm 9.2 \times 10^{-5}$
B	B270F	2012	528,923	$4.58 \times 10^{-1} \pm 4.5 \times 10^{-3}$	174.5 ± 1.7	$1.79 \times 10^{-2} \pm 8.9 \times 10^{-5}$
C	B270F	2013	595,771	$3.81 \times 10^{-1} \pm 3.8 \times 10^{-3}$	170.7 ± 1.7	$1.53 \times 10^{-2} \pm 7.6 \times 10^{-5}$
D	B270F	2013	210,814	$3.56 \times 10^{-1} \pm 3.5 \times 10^{-3}$	135.8 ± 1.3	$2.65 \times 10^{-2} \pm 1.3 \times 10^{-4}$
E	B340M	2014	518,640	$3.54 \times 10^{-1} \pm 3.5 \times 10^{-3}$	147.2 ± 1.4	$2.12 \times 10^{-2} \pm 1.0 \times 10^{-4}$
F	B340M	2014	367,100	$3.49 \times 10^{-1} \pm 3.4 \times 10^{-3}$	145.9 ± 1.4	$1.33 \times 10^{-2} \pm 6.6 \times 10^{-5}$
G	B450R	2015	670,803	$3.23 \times 10^{-1} \pm 3.2 \times 10^{-3}$	138.9 ± 1.3	$1.99 \times 10^{-2} \pm 9.9 \times 10^{-5}$
H	B450R	2016	856,794	$3.08 \times 10^{-1} \pm 3.0 \times 10^{-3}$	131.3 ± 1.3	$1.73 \times 10^{-2} \pm 8.6 \times 10^{-5}$
I	B450R	2018	938,933	$3.05 \times 10^{-1} \pm 3.0 \times 10^{-3}$	143.4 ± 1.4	$2.32 \times 10^{-2} \pm 1.1 \times 10^{-4}$
J	B450R	2020	93,449	$2.37 \times 10^{-2} \pm 2.3 \times 10^{-4}$	19.0 ± 0.2	$3.32 \times 10^{-2} \pm 1.6 \times 10^{-4}$

* Uncertainties based on the repeatability information of the analyzer specifications—HORIBA; PG-300 Series Portable Gas Analyzer.

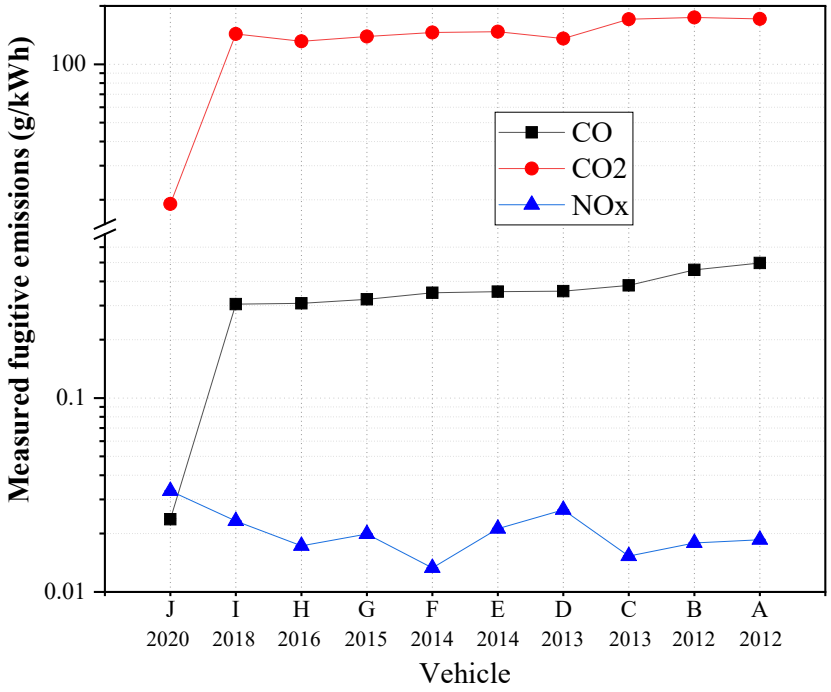

Figure 3. Influence of time on the evolution of fugitive emissions disregarding the mileage criterion.

5. Discussion

5.1. Influence of Mileage and Time Variables on Fugitive Emissions

Although the concentrations of pollutants in fugitive emissions, if analyzed individually, do not present clear behaviors with a tendency to increase, when analyzed without distinction of categories and engine models, the time variable shows a clear tendency for the concentrations to increase, Figure 3. For the three species analyzed, the running time of the motors, in displacement or steady state, can explain this direct relationship. The *CO* species appears with the highest rate of increase in concentration and tends to be influenced by both mileage traveled and time.

5.1.1. Carbon Dioxide (CO_2)

The concentration in CO_2 emissions tends to be influenced with increasing mileage of the engines. In both groups, there is a direct relationship between the explanatory variable mileage and the increase in concentration. This correlation is easily identified by analyzing the relations between the engines represented by samples A and D, belonging to the B270F group, which presented an increase of 20.7% in emissions between them. The engine represented by G increased its emissions by 86.3% compared to J. Likewise, the mileage of G was 90% higher than J, Table 6.

Table 6. Influence of mileage traveled on the evolution of (CO_2) emissions.

Vehicle	Model	Year	Mileage (km)	CO_2 (g/kWh)
A	B270F	2012	846,694	171.3 ± 1.7
B	B270F	2013	595,771	174.5 ± 1.7
C	B270F	2012	528,923	170.7 ± 1.7
D	B270F	2013	210,814	135.8 ± 1.3
E	B340M	2014	518,640	147.2 ± 1.4
F	B340M	2014	367,100	145.9 ± 1.4
G	B450R	2018	938,933	138.9 ± 1.3
H	B450R	2016	856,794	131.3 ± 1.3
I	B450R	2015	670,803	143.4 ± 1.4
J	B450R	2020	93,449	19.0 ± 0.2

5.1.2. Carbon Monoxide (CO)

Among the three species analyzed, the CO was the one that showed the highest and best relationship between engine mileage and increase in emission concentration. The Table 7 shows a clear tendency of evolution in the concentration of emissions as the engines suffer wear in function of the mileage. In all the groups analyzed it is possible to interpret these trends well. Engines represented by lines A, E and G increased their emission concentration by 28.4%, 1.4% and 92.6%, respectively, while the mileage increase for the same engines was 75.1%, 29.2% and 90.0%, respectively. This shows that fugitive CO emissions contribute more to GHG increases as engines gain mileage, compared to other analyzed species.

Table 7. Influence of mileage traveled on the evolution of (CO) emissions.

Vehicle	Model	Year	Mileage (km)	CO (g/kWh)
A	B270F	2012	846,694	$4.97 \times 10^{-1} \pm 4.97 \times 10^{-3}$
B	B270F	2013	595,771	$4.58 \times 10^{-1} \pm 4.58 \times 10^{-3}$
C	B270F	2012	528,923	$3.81 \times 10^{-1} \pm 3.81 \times 10^{-3}$
D	B270F	2013	210,814	$3.56 \times 10^{-1} \pm 3.56 \times 10^{-3}$
E	B340M	2014	518,640	$3.54 \times 10^{-1} \pm 3.54 \times 10^{-3}$
F	B340M	2014	367,100	$3.49 \times 10^{-1} \pm 3.49 \times 10^{-3}$
G	B450R	2018	938,933	$3.23 \times 10^{-1} \pm 3.23 \times 10^{-3}$
H	B450R	2016	856,794	$3.08 \times 10^{-1} \pm 3.08 \times 10^{-3}$
I	B450R	2015	670,803	$3.05 \times 10^{-1} \pm 3.05 \times 10^{-3}$
J	B450R	2020	93,449	$2.37 \times 10^{-2} \pm 2.37 \times 10^{-4}$

5.1.3. Nitrogen Oxides (NO_x)

The analyzed results show that the mileage of the engines has no direct influence to contribute to an increase in emissions of NO_x for any of the three groups, Table 8. Considering analyzed samples from engines of the same group, the engine represented by

A ran 75.1% more than engine D, but emitted 29.8% less NO_x. The relationship between samples G and J, also belonging to the same group, shows that engine J ran 90% less than engine G, but emitted 40% more NO_x. The second group, represented by the B340M model, shows consistency between the mileage and usage time variables, however, because it is only two samples it is not possible to perform a more elaborate analysis.

Table 8. Evolution of the Emissions of Oxides of NO_x as a function of mileage traveled.

Vehicle	Model	Year	Mileage (km)	NO_x (g/kWh)
A	B270F	2012	846,694	$1.86 \times 10^{-2} \pm 9.29 \times 10^{-5}$
B	B270F	2013	595,771	$1.79 \times 10^{-2} \pm 8.96 \times 10^{-5}$
C	B270F	2012	528,923	$1.53 \times 10^{-2} \pm 7.63 \times 10^{-5}$
D	B270F	2013	210,814	$2.65 \times 10^{-2} \pm 1.33 \times 10^{-4}$
E	B12M	2014	518,640	$2.12 \times 10^{-2} \pm 1.06 \times 10^{-4}$
F	B12M	2014	367,100	$1.33 \times 10^{-2} \pm 6.64 \times 10^{-5}$
G	B450R	2018	938,933	$1.99 \times 10^{-2} \pm 9.95 \times 10^{-5}$
H	B450R	2016	856,794	$1.73 \times 10^{-2} \pm 8.63 \times 10^{-5}$
I	B450R	2015	670,803	$2.32 \times 10^{-2} \pm 1.16 \times 10^{-4}$
J	B450R	2020	93,449	$3.32 \times 10^{-2} \pm 1.66 \times 10^{-4}$

5.2. Trend Analysis Using Response Surface Methodology (RSM)

By better explaining the phenomena involved in this investigation, the R Project for Statistical Computing [38] was used to model the relationships between the explanatory variables engine mileage and age for each of the analyzed species. The objective of this analysis is to identify whether there is a relationship with a growth trend in the concentrations of the species studied between the age and mileage of the engines. The mileage traveled and the age of manufacture of the engines up to 2020 were considered. Due to the liner behavior with constant variance and errors, as well as allowing optimization with analysis in more than one extreme as well as obtaining regression models that allow working with reduced numbers of control factors, the Response Surface Methodology (RSM) is the most appropriate concept that allows understanding the relationships between age and mileage run of engines. The initial form of data analysis in an experiment using the full regression model involving second order polynomial fitting factors is given by Equation (5).

$$y = \beta_0 + \sum_{i=1}^{q} \beta_i \chi_i + \sum_{i=1}^{q} \beta_{ii} \chi_i^2 + \sum_{i=1}^{q-1} \sum_{j=i+1}^{q} \beta_{ij} \chi_i \chi_j + \varepsilon \quad (5)$$

By using this methodology, and for the chemical species here analyzed, one can obtain the Equation (6) in order to represent the response surface. Note that in Equation (6), t_{usage} represent the engine/vehicle age (years) and the Mileage (km). For each species, a set of β_i will be obtained, depending of the statistical fit corresponding to the performed measurements.

$$\begin{aligned}[CO_2, CO, NO_x]|_{\text{fug-emissions(g/kWh)}} = \beta_0 + \beta_1 \times \left(\text{t}_{\text{usage}}|_{(\text{years})}\right) + \beta_2 \times \left(\text{Mileage}|_{(km)}\right) \\ + \beta_3 \times \left(\text{t}_{\text{usage}}|_{(\text{years})}\right)^2 + \beta_5 \times \left(\text{Mileage}|_{(km)}\right)^2 \\ + \beta_6 \times \left(\text{t}_{\text{usage}}|_{(\text{years})}\right) \times \left(\text{Mileage}|_{(km)}\right)\end{aligned} \quad (6)$$

5.2.1. Carbon Dioxide CO_2

The dispersion shown in Figure 4a,b shows that there were high emissions with emphasis on engines 4, 5 and 7. As the explanatory variables age and mileage are continuous, a polynomial model of degree 2 was considered and used Equation (6) to explain the phenomenon, identically and independently distributed with zero mean and constant variance.

It is observed in Figure 4c that engine 5 appears as an atypical value, positioning itself outside the reasonable region. Thus, after a first model adjustment, the observation referring to sample 5 was excluded. After this removal, we obtained the fitted model described in Equation (7), Figure 4d, with $R^2 = 0.90$, a correlation between measured data and theoretical modeling was observed. To further interpret the fitted model, the response surface plot of Figure 4e was generated. The optimum point at the upper end of the graph indicates that both high mileage and engine usage time have a direct influence in contributing to worsening CO_2 emissions.

$$CO_2|_{\text{fug}-\text{emissions(ppm)}} = -1.016 \times 10^{1} + 1.815 \times 10^{1}(\text{t}_{\text{usage}}) + 2.231 \times 10^{-4}(\text{Mileage}) \\ -8.778 \times 10^{-11}(\text{Mileage}) - 1.371 \times 10^{-5}(\text{t}_{\text{usage}})(\text{Mileage}) \quad (7)$$

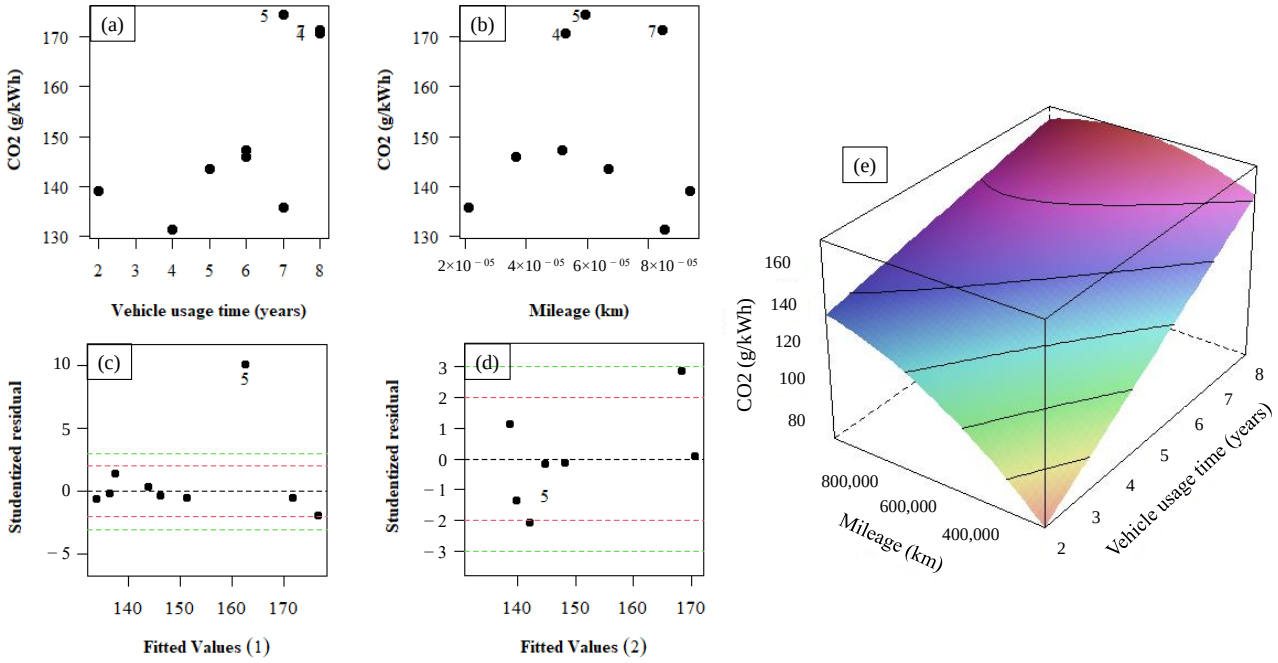

Figure 4. CO_2 fugitive emission behavior—adjustments of mileage-time relationships using a degree-2 polynomial. (**a**) First individual fit using equation 6 with mileage as the explanatory variable. Samples 4, 5, and 7 show high emissions rates; (**b**) Second individual fit using equation 6 with time of use as the explanatory variable. Similarly, samples 4, 5, and 7 show high emission rates; (**c**) A third fit applying all terms of the polynomial equation of degree 2 indicates an atypical value for sample 5, requiring a new fit; (**d**) The fourth and final adjustment after the removal of sample 5 brought improvements to the model; (**e**) Response surface shows an increasing trend for both explanatory variables (mileage and time of use).

5.2.2. Carbon Monoxide (*CO*)

High concentrations of fugitive emission these were also detected in samples 4 and 7 of the *CO* species. The Figure 5 shows the dispersion with emissions growth curve with usage time, Figure 5a, while this criterion is not very clear in the modeling by mileage, Figure 5b. Applying the polynomial model of degree 2 to explain the *CO* emission through Equation (6) and assigning the fitted values, was obtained Equation (8). The modeling showed good correlation between the measured data and theoretical modeling with $R^2 = 0.91$, Figure 5c. To interpret the fitted model, the response surface was generated Figure 5d. The optimum points at both ends of the response surface, even if not disregarding the saddle effect, indicates clear behavior of the influence of the explanatory variables mileage and time on increasing concentrations.

$$CO|_{\text{fug}-\text{emissions(g/kWh)}} = -8.178 \times 10^{-1} + 3.326 \times 10^{-1}\left(t_{\text{usage}}\right) - 1.641 \times 10^{-7}(\text{Mileage}) \\ -2.312 \times 10^{-2}\left(t_{\text{usage}}\right)^2 + 3.957 \times 10^{-13}(\text{Mileage})^2 \quad (8)$$

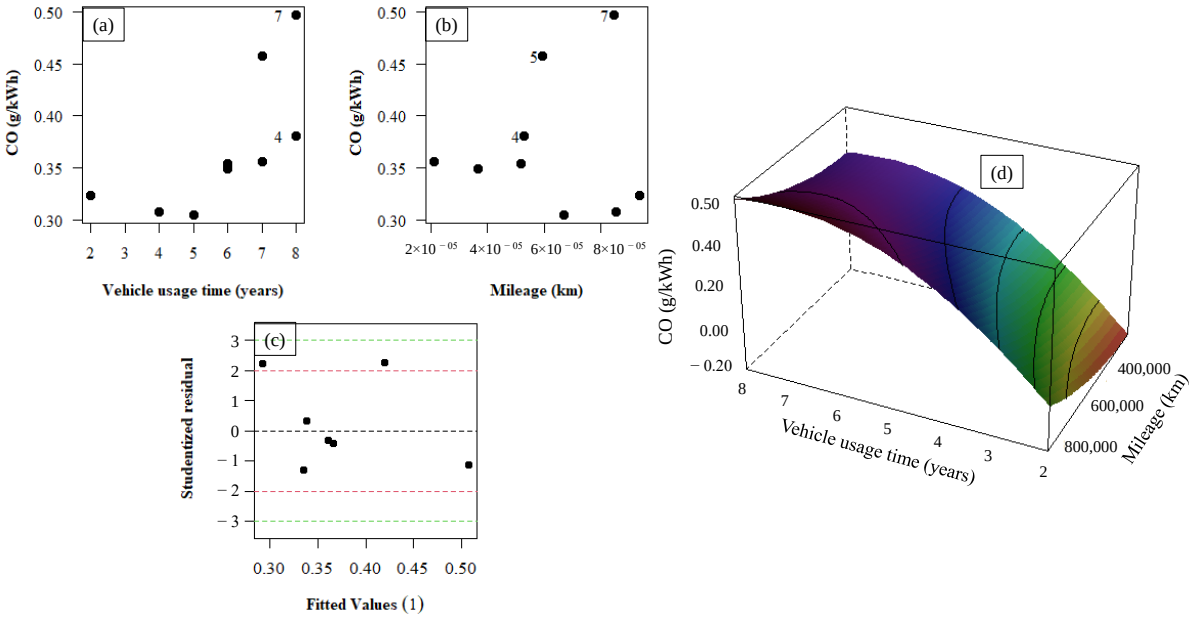

Figure 5. *CO* fugitive emission behavior—adjustments of mileage-time relationships using a degree-2 polynomial. (**a**) First individual fit using equation 6 with mileage as the explanatory variable. Samples 5, and 7 show high emissions rates; (**b**) Second individual fit using equation 6 with time of use as the explanatory variable. Similarly, samples 5, and 7 show high emission rates; (**c**) The third and last adjustment using all terms of the polynomial equation of degree 2 analyzed the correlation between the explanatory variables (mileage and time of use) brought improvements to the model; (**d**) The response surface shows an increasing trend in emissions with a higher degree for the time of use variable and a slightly increasing trend for mileage.

5.2.3. Nitrogen Oxide (NO_x)

Random behavior of the species NO_x in the analyses indicates no explicit relationship between the mileage and time variables, Figure 6a,b. Although there is no apparent correlation between the two variables, a polynomial model of degree 2 was considered, Equation (9) to explain the emission of NO_x. Even adjusted, the model did not meet the assumptions required for good optimization, however, there is a point of influence observed in Figure 6c positioning itself outside the reasonable. After the removal of this point, another point appeared, also outside the reasonable region, as we do not have many points in the sample, the removal of more points would compromise the reliability of the adjusted model. Thus, it was concluded that no information supports accuracy in the analysis of the species NO_x. The statistical environment output of RStudio makes it literally clear that the minimum model requirements for a significant response are not met, because none of the model parameters are considered significant. With P_{value} calculated at 0.7942, far above the parameters indicated as accepted that range between ($0.01 <= P < 0.05$) and determination coefficient at R^2 = 0.4306, considered too low, one then summarizes the unreliability in the significance of the data for this species of gas.

$$NO_x = \beta_0 + \beta_1 \times \left(t_{\text{usage}}\right) + \beta_2 \times (\text{Mileage}) + \beta_3 \times \left(t_{\text{usage}}\right) \times (\text{Mileage}) \\ +\beta_4\left(t_{\text{usage}}\right)^2 + \beta_5(\text{Mileage})^2 + \varepsilon \quad (9)$$

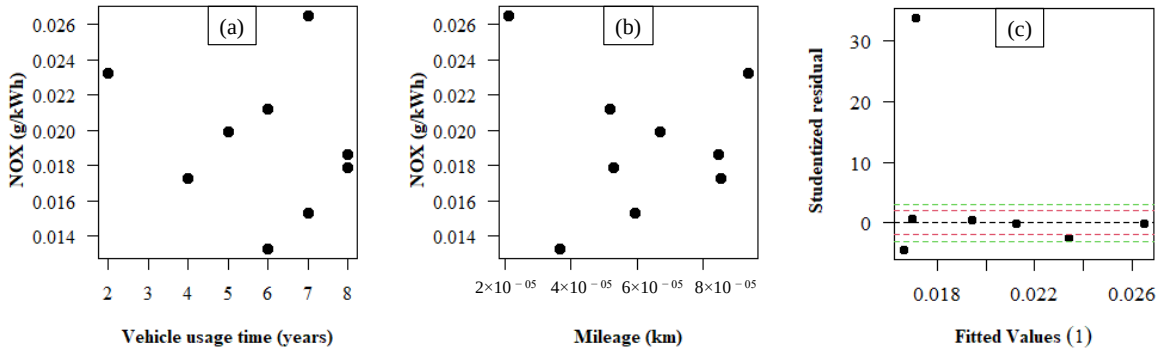

Figure 6. NO_x fugitive emission behavior—adjustments of mileage-time relationships using a degree-2 polynomial. (**a**) First individual fit using equation 9 with mileage as the explanatory variable; (**b**) Second individual fit using equation 9 with time of use as the explanatory variable; (**c**) The third and last adjustment using all terms of the polynomial equation of degree 2 analyzed the correlation between the explanatory variables (mileage and time of use). There was no acceptable correlation and no adjustment to the model was possible.

6. Conclusions

It is noted that the study results align with the main objectives reported in the abstract and introduction. Fugitive emissions were detected in the samples analyzed in the laboratory, Table 5. Considering the official results reported by the laboratory analyses in mol/mol(%), applying the conversion factor described in section 4, the measured values range between (3.000–27.500 ppm) for samples B and J, respectively, which indicates a magnitude far above the current average of 418.36 ppm (18 February 2023) reported in real-time by the Global Monitoring Laboratory observatory [39]. The results showed that the CO and NO_x species presented average concentrations within the range established by the current legislation that regulates pollutant emissions in heavy-duty vehicles. On a scale of (0 to 1), where 0 represents no emission and 1 is the maximum limit established, the average CO concentration was 0.335 while the average NO_x concentration was 0.021. The positive results, from the point of view of comparison with the current legislation, are justified and were exhaustively clarified in the introduction, however, the preponderant factor analyzed refers to the biased conditions of increase in concentrations with the increase in the time of use and mileage of the engines. The average concentration of fugitive CO_2 emissions was 137.9 $\pm$ 1.7 g/kWh. After the first adjustment and removal of sample 5, Figure 4c, the model has fitted again and showed optimal interaction with low variance whose R^2 determination index of 0.90 and 100% of the samples placing within the reasonable region, Figure 4d demonstrates this behavior, which can also be observed by analyzing the response surface graph in Figure 4e where it is possible to see a clear tendency for fugitive emissions to increase with both increasing usage time and mileage of the engines. Showing good interaction between the uncontrolled variables, mileage and usage time, and a coefficient of determination R^2 of 0.91, the fugitive emissions of *CO* showed adjusted values whose behavior differs from the other analyzed species. In the scatter plot shown in Figure 5a the time factor is the determinant for the increase of *CO* emissions, while Figure 5b does not present clarity about the possible influence of mileage of the engines in the contribution of fugitive emissions, behavior also observed in the analyzed response surface, Figure 5d. For the species NO_x, analysis of the scatter plot Figure 6a,b show that the interaction between the explanatory variables mileage and usage time is not explicitly evidenced. With P_{value} of 0.860 and 0.864 for the linear term, 0.945 and 0.465 for the quadratic term as well as 0.758 for interaction, determination index R^2 of 43%, it can be concluded that the model fits did not meet the minimum assumptions and requirements for statistically significant responses. It should be noted that there are many possible influencing factors/parameters that can indicate the direct influence on higher CO_2 and *CO* fugitive emissions. First, the higher the

mileage the higher the chances of increasing the leakage area throughout gases may exit (as fugitive emissions), because of the natural degradation of pipeline materials. Note that this is not an isolated effect on the mileage, the same can be expected when looking at the engine usage time. Another important aspect here is concerning the vehicle's technical-mechanical state. There are many factors that can influence this tendency. All the phenomenological process preceding the combustion process has a strong effect, for example, if cavitation is present in the fuel injector, the spray behavior will be affected, especially in terms of spray cone angle, penetration, and dispersion [40–43]. Cavitation could appear in the fuel injector after several times of use (directly involving mileage and usage time). It is known that transportation industries are enforced to implement routinary and rigorously maintenance technical-mechanical prevention programs, so it should be expected that all the vehicles analyzed here undergo those prevention programs, however, we do not have access to that information. With the exception of the CO_2 species, it should be noted that the emission levels measured in this research were "within" Euro V regulations, results that are in the opposite direction of what is expected in terms of vehicular fugitive emissions, considering that the sample locations were selected at points before after-treatment of the exhaust gas systems. This issue raises several concerns related to fugitive emission analysis and measurement techniques focused on vehicle systems, due to the large number of variables involved in the process, (technical-mechanical condition of the vehicle, effective leak area, encapsulation sampling process) among those previously mentioned.

Author Contributions: Conceptualization, A.C.C.; P.H.S. and C.M.G.A.; Methodology, A.C.C. and L.R.C.; Software, V.J. and L.R.C.; Validation, A.C.C.; P.H.S.; C.M.G.A. and L.R.C.; Formal analysis, A.C.C. and V.J. and L.R.C.; Investigation, A.C.C. and L.R.C.; Resources, A.C.C.; Writing—original draft preparation, A.C.C.; Writing—review and editing, L.R.C.; Visualization, A.M.S.d.C.; Supervision, A.C.C. and L.R.C.; Funding acquisition, A.C.C. and C.M.G.A. All authors have read and agreed to the published version of the manuscript.

Funding: CAPES and CNPq. The experiments and laboratory analyses where funded by Antonio C. Caetano.

Informed Consent Statement: Not applicable.

Acknowledgments: The authors would like to acknowledge the support of (a) Asatur Transportes e Turismo LTDA, Renildo Lima and Maria Helena (b) Eucatur Empresa União Cascavel de Transporte e Turismo LTDA. José Roberto Silva, (c) Viação São Pedro Transportes Urbano de Passageiros LTDA, Marcelo Alves, and (d) White Martins Brasil, Cleber Costa.

Conflicts of Interest: The authors declare no conflict of interest

References

1. IPCC. *Global Warming of 1.5 °C: IPCC Special Report on Impacts of Global Warming of 1.5 °C above Pre-industrial Levels in Context of Strengthening Response to Climate Change, Sustainable Development, and Efforts to Eradicate Poverty*, 1st ed.; Cambridge University Press: Cambridge, UK, 2022. [CrossRef]
2. The United Nations. *Report of the United Nations Conference on the Human Environment*; Technical Report; The United Nations: Stockholm, Sweden, 1972.
3. The United Nations. *Report of the United Nations Conference on Environment and Development, Rio De Janeiro, Brazil, 3–14 June 1992; Volume 1, Resolutionsadopted By The Conference*; Technical Report; The United Nations: Rio de Janeiro, Brazil, 1992.
4. United Nations Climate Change. *The Paris Agreement—UNFCCC*; Technical Report; The United Nations: Paris, France, 2015.
5. United Nations Climate Change. Greenhouse Gas Inventory Data—Time Series—Annex I—GHG total without LULUCF, in kt CO_2 Equivalent. https://di.unfccc.int/ (accessed on 1 November 2022).
6. The European Commission. *Energy, Transport and Environment Statistics—2020 Edition*; Technical Report; The European Commission, European Union: Stockholm, Sweden, 2020. [CrossRef]
7. Intergovernmental Panel on Climate Change. *Climate Change 2022: Mitigation of Climate Change*; Technical Report; Working Group III Contribution to the Sixth Assessment Report of the Intergovernmental Panel on Climate Change; Cambridge University Press: Cambridge, UK; New York, NY, USA, 2022. [CrossRef]
8. Intergovernmental Panel on Climate Change—IPCC. 2006 IPCC Guidelines for National Greenhouse Gas Inventories—Volume 1—General Guidance and Reporting Publications—IPCC-TFI, 2006. Chapter 8—Reporting Guidance and Tables. https://www.ipcc-nggip.iges.or.jp/public/2006gl/vol1.html (accessed on 1 November 2022).

9. Intergovernmental Panel on Climate Change. *Climate Change 2022: Impacts, Adaptation and Vulnerability*; Technical Report; Working Group II Contribution to the Sixth Assessment Report of the Intergovernmental Panel on Climate Change; Cambridge University Press: Cambridge, UK; New York, NY, USA, 2022. [CrossRef]
10. Laconde, T. Fugitive emissions: A blind spot in the fight against climate change. In *Climate Chance—2018 Annual Report, Global Observatory On Non-State Climate Action*; Climate Chance Association: Rue du Faubourg Saint-Antoine, Paris, 2018. https://www.climate-chance.org/en/2018report/ (accessed on 1 November 2022).
11. Solazzo, E.; Crippa, M.; Guizzardi, D.; Muntean, M.; Choulga, M.; Janssens-Maenhout, G. Uncertainties in the Emissions Database for Global Atmospheric Research (EDGAR) emission inventory of greenhouse gases. *Atmos. Chem. Phys.* **2021**, *21*, 5655–5683. [CrossRef]
12. Effiong, M.O.; Okoye, C.U.; Nweze, N.J. Sectoral contributions to carbon dioxide equivalent emissions in the nigerian economy. *Int. J. Energy Econ. Policy* **2019**, *10*, 456–463. [CrossRef]
13. Hmiel, B.; Petrenko, V.V.; Dyonisius, M.N.; Buizert, C.; Smith, A.M.; Place, P.F.; Harth, C.; Beaudette, R.; Hua, Q.; Yang, B.; et al. Preindustrial 14CH4 indicates greater anthropogenic fossil CH4 emissions. *Nature* **2020**, *578*, 409–412. [CrossRef] [PubMed]
14. United Nations Framework Convention on Climate Change—UNFCCC. *Measurements for Estimation of Carbon Stocks—In Afforestation and Reforestation Project Activities under the Clean Development Mechanism—A Field Manual*, 1st ed.; Platz der Vereinten Nationen: Bonn, Germany, 2015. http://www.unfccc.int (accessed on 1 November 2022).
15. Singh, A.; Unnikrishnan, S.; Naik, M.; Sayanekar, S. CDM implementation towards reduction of fugitive greenhouse gas emissions. *Environ. Dev. Sustain.* **2019**, *21*, 569–586. [CrossRef]
16. Nogueira, T.; Dominutti, P.A.; Vieira-Filho, M.; Fornaro, A.; Andrade, M.d.F. Evaluating Atmospheric Pollutants from Urban Buses under Real-World Conditions: Implications of the Main Public Transport Mode in São Paulo, Brazil. *Atmosphere* **2019**, *10*, 108. [CrossRef]
17. The European Environment Agency (EEA). *EMEP/EEA Air Pollutant Emission Inventory Guidebook—European Environment Agency*; Publication Office of the European Union: Luxembourg, 2019. [CrossRef]
18. Savickas, D.; Steponavičius, D.; Špokas, L.; Saldukaitė, L.; Semenišin, M. Impact of Combine Harvester Technological Operations on Global Warming Potential. *Appl. Sci.* **2021**, *11*, 8662. [CrossRef]
19. Soares, P.H.; Monteiro, J.P.; Freitas, H.F.; Zenko Sakiyama, R.; Andrade, C.M. Platform for monitoring and analysis of air quality in environments with large circulation of people. *Environ. Prog. Sustain. Energy* **2018**, *37*, 2050–2057. [CrossRef]
20. Soares, P.H.; Monteiro, J.P.; de Freitas, H.F.S.; Ogiboski, L.; Vieira, F.S.; Andrade, C.M.G. Monitoring and Analysis of Outdoor Carbon Dioxide Concentration by Autonomous Sensors. *Atmosphere* **2022**, *13*, 358. [CrossRef]
21. Official Journal of the European Union. Regulation (EC) No 715/2007 of the European Parliament and of the Council of 20 June 2007. Doc ID: L:2007:171:TOC. https://eur-lex.europa.eu (accessed on 1November 2022).
22. Jenkins, D.G.; Quintana-Ascencio, P.F. A solution to minimum sample size for regressions. *PLoS ONE* **2020**, *15*, e0229345. [CrossRef] [PubMed]
23. Yoo, H.; Lee, J.W. Sample size calculation based on discrete Weibull and zero-inflated discrete Weibull regression models. *Commun. Stat.—Simul. Comput.* **2022**, *51*, 7180–7193. [CrossRef]
24. National Service Center for Environmental Publications (NSCEP). *Protocol for Equipment Leak Emission Estimates*; Report EPA-453/R-95-017; NSCEP: Research Triangle Park, NC, USA, 1995
25. Hennigan, S. Method 21 monitors fugitive emissions. *Environ. Prot.* **1993**, *4*, 22–31. https://www.osti.gov/biblio/249852 (accessed on 1 October 2022).
26. Wilson, A. New Optical Gas-Imaging Technology for Quantifying Fugitive-Emission Rates. *J. Pet. Technol.* **2016**, *68*, 78–79. [CrossRef]
27. Abdel-Moati, H.; Morris, J.; Zeng, Y.; Kangas, P.; McGregor, D. *New Optical Gas Imaging Technology for Quantifying Fugitive Emission Rates*; OnePetro: Doha, Qatar, 2015. [CrossRef]
28. Asiamah, N.; Conduah, A.K.; Eduafo, R. Social network moderators of the association between Ghanaian older adults' neighbourhood walkability and social activity. *Health Promot. Int.* **2021**, *36*, 1357–1367. [CrossRef] [PubMed]
29. Maas, R.P.P.W.M.; Teerenstra, S.; Toni, I.; Klockgether, T.; Schutter, D.J.L.G.; van de Warrenburg, B.P.C. Cerebellar Transcranial Direct Current Stimulation in Spinocerebellar Ataxia Type 3: A Randomized, Double-Blind, Sham-Controlled Trial. *Neurotherapeutics* **2022**, *19*, 1259–1272. [CrossRef] [PubMed]
30. Yurdakoş, K.; Sarihan, M. Irrational use of medicines: The magnitude of economic loss due to wasted medicines that cannot be prescribed, sold and used in an instant optimized manner. *Mersin Üniv. Sağlık Bilim. Derg.* **2022**, *15*, 517–530. [CrossRef]
31. VOLVO do Brasil. Volvo B270F Charter Specifications, 2022. https://www.volvobuses.com/br/Rodoviario/b270f-fretamento/specifications.html (accessed on 1 October 2022).
32. VOLVO do Brasil. Volvo B340M Charter Specifications, 2022. https://www.volvobuses.com/br/Urbano/b340m-articulado-biarticulado/specifications.html (accessed on 1 October 2022).
33. VOLVO do Brasil. Volvo B11R Charter Specifications, 2022. https://www.volvobuses.com/en/coaches/chassis/volvo-b11r/specifications.html (accessed on 1 October 2022).
34. Vergel-Ortega, M.; Valencia-Ochoa, G.; Duarte-Forero, J. Experimental study of emissions in single-cylinder diesel engine operating with diesel-biodiesel blends of palm oil-sunflower oil and ethanol. *Case Stud. Therm. Eng.* **2021**, *26*, 101190. [CrossRef]

35. Ağbulut, U.; Sarıdemir, S.; Albayrak, S. Experimental investigation of combustion, performance and emission characteristics of a diesel engine fuelled with diesel–biodiesel–alcohol blends. *J. Braz. Soc. Mech. Sci. Eng.* **2019**, *41*, 389. [CrossRef]
36. Kopseak, H.; Pandur, Z.; Bačić, M.; Zečić, u.; Nevečerel, H.; Lepoglavec, K.; Šušnjar, M. Exhaust Gases from Skidder ECOTRAC 140 V Diesel Engine. *Forests* **2022**, *13*, 272. [CrossRef]
37. Soca-Cabrera, J.R. Diesel engine emissions off road. Case Volskwagen ADG 1.9 L SDI. *Rev. Cienc. Técnicas Agropecu.* **2020**, *29*, 15–23.
38. R Core Team. *R: A Language and Environment for Statistical Computing*; R Foundation for Statistical Computing: Vienna, Austria, 2021.
39. Global Monitoring Laboratory. Carbon Cycle Greenhouse Gases. 2023. Available online: https://gml.noaa.gov/ccgg/ (accessed on 18 February 2023).
40. Baumgarten, C. *Mixture Formation in Internal Combustion Engine*; Heat, M.T., Ed.; Springer: Berlin/Heidelberg, Germany, 2006. [CrossRef]
41. Adão, W.B.; Cancino, L.R. Spray Behavior on Compression Ignition Internal Combustion Engines: A CFD Analysis of Cavitation in the Fuel Injector. In Proceedings of the COBEM 2019—25th ABCM International Congress of Mechanical Engineering, Uberlândia, Brazil, 20–25 October 2019; p. COB–2019–2161.
42. Henschel, J.A., Jr.; Cancino, L.R. Numerical Analysis of Fuel Spray Angle on the Operating Parameters in a Locomotive Diesel Engine. In Proceedings of the COBEM 2019—25th ABCM International Congress of Mechanical Engineering, Uberlândia, Brazil, 20–25 October 2019; p. COB–2019–1642.
43. Rotter, D.V.; Hackbarth, G.Z.; Henschel, J.A., Jr.; Cancino, L.R. Spray and Combustion Behavior in a Locomotive Engine Using Diesel/Biodiesel Blends: A CRFD Analysis. In Proceedings of the COBEM 2021—26th International Congress of Mechanical Engineering, Online, 22–26 November 2021; p. COB–2021–0706.